



Location of the internal carotid artery and ophthalmic artery segments for non-invasive intracranial pressure measurement by multi-depth TCD

Yasin Hamarat ^a, Mantas Deimantavicius^a, Evaldas Kalvaitis^a, Lina Siaudvytyte^b, Ingrida Januleviciene^b, Rolandas Zakelis^a and Laimonas Bartusis ^a

^aHealth Telematics Science Institute, Kaunas University of Technology, Kaunas, Lithuania; ^bEye Clinic, Lithuanian University of Health Sciences, Kaunas, Lithuania

ABSTRACT

The aim of the present study was to locate the ophthalmic artery by using the edge of the internal carotid artery (ICA) as the reference depth to perform a reliable non-invasive intracranial pressure measurement via a multi-depth transcranial Doppler device and to then determine the positions and angles of an ultrasonic transducer (UT) on the closed eyelid in the case of located segments. High tension glaucoma (HTG) patients and healthy volunteers (HVs) undergoing non-invasive intracranial pressure measurement were selected for this prospective study. The depth of the edge of the ICA was identified, followed by a selection of the depths of the IOA and EOA segments. The positions and angles of the UT on the closed eyelid were measured. The mean depth of the identified ICA edge for HTG patients was 64.3 mm and was 63.0 mm for HVs ($p = 0.21$). The mean depth of the selected IOA segment for HTG patients was 59.2 mm and 59.3 mm for HVs ($p = 0.91$). The mean depth of the selected EOA segment for HTG patients was 48.5 mm and 49.8 mm for HVs ($p = 0.14$). The difference in the located depths of the segments between groups was not statistically significant. The results showed a significant difference in the measured UT angles in the case of the identified edge of the ICA and selected ophthalmic artery segments ($p = 0.0002$). We demonstrated that locating the IOA and EOA segments can be achieved using the edge of the ICA as a reference point.

Abbreviations: OA: ophthalmic artery; IOA: intracranial segments of the ophthalmic artery; EOA: extracranial segments of the ophthalmic artery; ICA: internal carotid artery; UT: ultrasonic transducer; HTG: high tension glaucoma; SD: standard deviation; ICP: intracranial pressure; TCD: transcranial Doppler

ARTICLE HISTORY

Received 2 June 2017
Accepted 20 September 2017

RESPONSIBLE EDITOR

Hani Benamer, University of Birmingham College of Medical and Dental Sciences, UK

KEYWORDS

Ultrasonic Doppler technology; internal carotid artery; location of the ophthalmic artery; intracranial pressure; non-invasive measurement

1. Introduction

Intracranial pressure (ICP) measurement is clinically important to many neurological diseases [1–3] and some neurosurgical conditions [4–6]. ICP measurement can also be clinically important in ophthalmology to assess the progress of glaucoma disease [7–9], in nephrology during haemodialysis sessions [10] and even in gynaecology during laparoscopic surgeries [11]. Unfortunately, the absolute value of the ICP is measured using invasive techniques in clinical practice.

Transcranial Doppler (TCD) was introduced by Aaslid in 1982. Since then, TCD has become an attractive tool to assess the cerebrovascular tree [12,13]. TCD-based methods can estimate ICP non-invasively via blood flow velocity parameters that are obtained from the cerebral arteries [14]. However, nearly all ICP assessment approaches are correlation-based or model-based; therefore, the absolute value of the

ICP cannot be measured because patient-specific calibration is required for such measurement methods.

A novel TCD-based non-invasive absolute ICP measurement method that does not require patient-specific calibration has been developed [15]. To make a reliable non-invasive measurement of the ICP with this method, the operator must manually find correct depths of the intracranial (IOA) and extracranial (EOA) segments of the ophthalmic artery (OA) using a multi-depth TCD. Clinical studies have already shown applicable accuracy, precision, diagnostic sensitivity and specificity of the non-invasive ICP measurement method [16,17].

Normally, the ophthalmic artery is the first branch of the larger internal carotid artery (ICA) [18]. The pulse wave shape in the ICA is usually different than in the OA. Thus, it is easy to distinguish the ICA from the OA via TCD spectral patterns [19]. There are some published results of OA anatomical studies [18,20–22]. The following summarises the results of these studies:

- (1) The distance between the OA branching point from the ICA up to the point where the OA pierces the dura mater is individual to each person. The potential range of the IOA distances from the ICA is 0.5–9.5 mm. The range of depths of the selected IOA segment with a low probability to overlap/cross the area of the dura mater should be 3–5 mm away from the edge of the ICA.
- (2) The possible length range of the OA that extends from the dura mater up to the apex of the orbit is 3.9–7.0 mm. To select the correct depth of the extracranial segment of the OA, the range of depth of the selected EOA segment with a low probability to overlap/cross the area of the dura mater and with the high probability that the OA segment would be in the intraorbital part and should be 8–12 mm away from the IOA.

Several publications have focused on the depths of the ICA and OA measured by TCD from the external surface of the closed eyelid. Naqvi et al. found that the depth of the ICA is 65–80 mm and that of the OA is 45–55 mm [13]. Alexandrov et al. showed that the ICA depth was 58–65 mm [23]; Kassab et al. reported an OA depth of 40–60 mm [23,24]. Thus, the literature agrees on an ICA depth between 58 and 80 mm [13,23–25], whereas the depth of the OA is between 40 and 60 mm [13,24,25]. Although these publications show a possible depth range of the ICA and the OA, none has mentioned the depth ranges of the edge of the ICA or the depth range of the IOA and EOA, which would be advantageous to the operator who locates the IOA and EOA segments before non-invasive ICP measurement can be initiated.

The main aim of this study was to prospectively locate the depth range of the ICA edge followed by a simultaneous location of the depths of the IOA and EOA segments to perform a reliable non-invasive ICP measurement.

2. Methods

2.1. Patient eligibility

Our prospective study was conducted in the Eye Clinic at the Hospital of the Lithuanian University of Health Sciences and the Health Telematics Science Institute of the Kaunas University of Technology between July 2013 and March 2016.

High tension glaucoma (HTG) patients and healthy volunteers (HVs) undergoing non-invasive intracranial pressure measurement were selected. The exclusion criteria were as follows: younger than 18 years, pregnant or nursing females, subjects with uncontrolled systemic diseases, and subjects with a history of

allergy to local anaesthetics, orbital/ocular trauma or other diseases.

2.2. Standard protocol approval, registration, and patient consent

The protocol of this prospective study was approved by the Kaunas Regional Bioethics Committee (Registration No. BE – 2 – 41). Patients' written consent was obtained in accordance with the Declaration of Helsinki (BMJ 1991; 302: 1194).

2.3. Data collection

A Vittamed 205 (Kaunas, Lithuania) device with the following parameters was used for the TCD examination: ultrasound probe central frequency of 2 MHz, sample volume size equal to 3 mm, and power levels matching approved ultrasound devices.

The head frame designed for the non-invasive intracranial pressure measurement was fitted onto the heads of healthy volunteers or glaucoma patients for convenient ultrasonic transducer positioning and orientation (Figure 1(b,c)). First, the depth where the OA branches from the ICA (edge of ICA) should be identified. By using the edge of the ICA as a reference depth, the intracranial and extracranial segments of the OA can be selected with respect to anatomical studies that have already defined the probable range of OA depths [20–22] and then followed by a reliable non-invasive measurement of ICP. Depths of the located segments from the closed eyelid were recorded in millimetres. Positions of the circular ultrasonic transducer of 14 mm in diameter on the closed eyelid were recorded in the case of the identified edge of the ICA, and the IOA selected simultaneously with the EOA. An example of the marked positions of the UT on the closed eyelid (schematic representation) is shown in Figure 1(a). We estimated the average orientation of the UT on the closed eyelid in the case of the identified edge of the ICA, and the IOA selected simultaneously with the EOA. The measured alpha and beta angles of the UT are depicted in Figure 1(b,c), respectively.

2.4. Statistical analysis

The statistical analysis was performed using MedCalc software (version 16.4.3; MedCalc Software, Ostend, Belgium). The distance between the edge of the ICA and the IOA segment (ICA-IOA) as well as the distance between the IOA and EOA segments (IOA-EOA) were calculated. The analysis of the quantitative variables included a calculation of the mean and standard deviation (SD) and a comparison of the means between two groups: HTG patients and HVs.

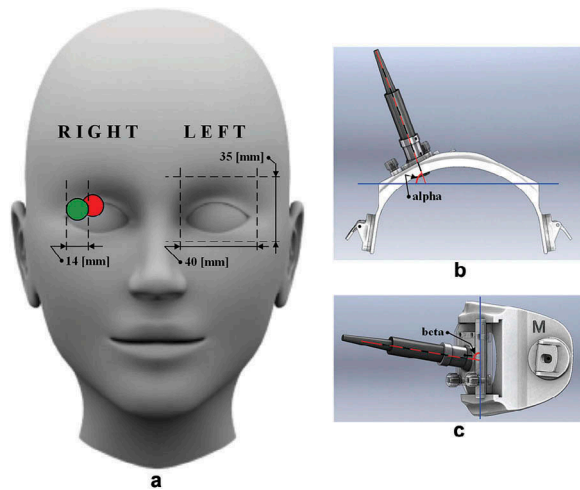


Figure 1. Schematic representation of the measurements of positions and angles of an ultrasonic transducer (UT) on the closed eyelid. (a) Example of the relative positions of the UT of 14 mm in diameter on the closed eyelid in the case of the identified edge of the internal carotid artery (red circle on the right eye) and the depth of intracranial segment of ophthalmic artery selected simultaneously with the depth of the extracranial segment of the ophthalmic artery (green circle on the right eye). The average adult human orbit geometry (height and width) is depicted on the left eye. (b) Schematic representation of the head frame top view used for UT positioning and orientation. Angle alpha, which was measured between the longitudinal axis of the UT (red dashed line) and the frontal axis of a human head (blue solid line), is depicted. (c) Schematic representation of the head frame sideview used for UT positioning and orientation. Angle beta, which was measured between the longitudinal axis of the UT (red dashed line) and the vertical axis of a human head (blue solid line), is depicted.

Differences were analysed using the *t*-test. The level of $p < 0.05$ was considered significant.

The window of the relative UT position on the closed eyelid in the case of the identified ICA edge and the IOA depth selected simultaneously with the EOA depth were estimated using the average adult human orbit geometry [26,27].

3. Results

Twenty-five HTG patients and 23 HVs were included. The data were collected on HTG patients – there were 14 right eyes and 19 left eyes (in total, 33 eyes) – and on HVs – there were 20 right eyes and 13 left eyes (in total, 33 eyes).

In this study, the probability of finding an IOA segment at a distance not more than 5 mm from the identified ICA edge was 74% (49 cases from 66). However, the maximum distance between the identified ICA edge and the selected IOA segment was 9 mm. This was observed in four cases. In one case, it was 8 mm; in five cases, 7 mm; and in seven cases, 6 mm. With some exceptions, this supports the proposed method that the IOA segment has to be found

at a distance 3–5 mm away from the identified ICA edge. The probability of finding an EOA segment 8–12 mm from the selected IOA segment was 92% (61 cases from 66). In one case, it was 7 mm, twice it was 13 mm, once it was 15 mm, and once it was 16 mm. With some rare exceptions, this suggests that the EOA segment is 8–12 mm away from the selected IOA segment.

The depths of the edge of the ICA and IOA with the EOA, the calculated distances between the edge of the ICA and the IOA segment (ICA edge–IOA), and the calculated distances between the IOA and EOA segments (IOA–EOA) for HTG patients are presented in Table 1. Data from HVs are presented in Table 2. The mean depth of the ICA edge for HTG patients was 64.3 mm (SD = 4.4 mm); it was 63.0 mm (SD = 4.0 mm) for HVs. The difference between groups was not statistically significant ($p = 0.21$). The differ-

Table 1. Depth and distance data of the located edge of the internal carotid artery and segments of ophthalmic artery in high tension glaucoma patients.

No. of glaucoma patients	Eye	ICA edge, mm	IOA, mm	EOA, mm	ICA edge–IOA, mm	IOA–EOA, mm
1	L	60	55	44	5	11
2	R	72	65	50	7	15
	L	60	57	46	3	11
3	R	61	58	46	3	12
	L	58	55	47	3	8
4	R	64	59	49	5	10
5	R	60	57	47	3	10
	L	60	57	47	3	10
6	R	60	58	47	2	11
7	L	65	58	47	7	11
8	L	64	57	47	7	10
9	L	60	54	43	6	11
10	L	68	62	46	6	16
11	R	62	56	44	6	12
12	L	64	57	45	7	12
13	R	62	59	49	3	10
	L	62	58	48	4	10
14	R	62	56	45	6	11
	L	68	59	49	9	10
15	R	73	69	58	4	11
	L	65	62	52	3	10
16	L	65	60	50	5	10
17	R	66	57	47	9	10
	L	61	56	43	5	13
18	R	70	62	53	8	9
19	L	60	57	44	3	13
20	L	74	65	55	f	10
21	R	68	59	51	9	8
22	L	68	64	56	4	8
23	R	59	57	47	2	10
24	R	70	64	54	6	10
	L	70	64	54	6	10
25	L	62	60	51	2	9
MEAN		64.3	59.2	48.5	5.2	10.7
SD		4.4	3.5	3.8	2.2	1.7

Data are presented for each high tension glaucoma patient separately, including all 25 patients and 33 examined eyes. Means \pm SD are also presented. R indicates the right eye; L, left eye; ICA edge, identified depth of the internal carotid artery edge from the closed eyelid; IOA, selected depth of the intracranial segment of the ophthalmic artery from the closed eyelid; EOA, selected depth of the extracranial segments of the ophthalmic artery from the closed eyelid; ICA edge–IOA, distance between the identified internal carotid artery edge and the selected intracranial segment of the ophthalmic artery; IOA–EOA, distance between the selected intracranial and extracranial segments of the ophthalmic artery.

Table 2. Depth and distance data of the located edge of the internal carotid artery and segments of the ophthalmic artery in healthy volunteers.

No. of healthy volunteers	Eye	ICA edge, mm	IOA, mm	EOA, mm	ICA edge–IOA, mm	IOA–EOA, mm
1	R	62	59	49	3	10
	L	56	53	45	3	8
2	R	60	57	48	3	9
	L	58	55	45	3	10
3	R	62	58	48	4	10
	L	64	60	50	4	10
4	R	66	61	51	5	10
	L	58	55	45	3	10
5	R	58	55	45	3	10
	L	58	54	44	4	10
6	R	69	65	55	4	10
	L	67	62	52	5	10
7	R	61	58	48	3	10
	L	54	51	42	3	9
8	R	70	65	55	5	10
	L	71	66	56	5	10
9	R	64	62	52	2	10
	L	64	60	50	4	10
10	R	64	61	50	3	11
	L	65	59	52	6	7
11	R	62	57	49	5	8
12	L	65	61	50	4	11
13	L	62	59	49	3	10
14	R	62	59	50	3	9
15	L	64	61	51	3	10
16	R	61	58	48	3	10
17	R	62	59	51	3	8
18	R	66	63	53	3	10
19	R	65	61	52	4	9
20	R	71	64	55	7	9
21	R	64	61	51	3	10
22	R	61	58	49	3	9
23	R	64	61	52	3	9
MEAN		63.0	59.3	49.8	3.7	9.6
SD		4.0	3.4	3.3	1.1	0.9

Data are presented for each healthy volunteer separately, including all 23 volunteers and 33 examined eyes. Means \pm SD are also presented. R indicates right eye; L, left eye; ICA edge, identified depth of the internal carotid artery edge from the closed eyelid; IOA, selected depth of the intracranial segment of the ophthalmic artery from the closed eyelid; EOA, selected depth of the extracranial segments of the ophthalmic artery from the closed eyelid; ICA edge–IOA, distance between the identified internal carotid artery edge and the selected intracranial segment of the ophthalmic artery; IOA–EOA, distance between the selected intracranial and extracranial segments of the ophthalmic artery.

ence between the selected mean depth of the IOA segment for HTG patients [59.2 mm (SD = 3.5 mm)] and HVs [59.3 mm (3.4 mm)] was not statistically significant ($p = 0.91$). The difference between the selected mean depth of the EOA segment for HTG patients [48.5 mm (SD = 3.8 mm)] and HVs [49.8 mm (SD = 3.3 mm)] was not statistically significant ($p = 0.14$).

Distribution graphs of identified depths of the edge of the ICA as well as the selected depth of IOA and EOA segments for graphical assessment are presented in Figure 2 (data collected on both groups are included). Distribution graphs of the calculated distances between the identified segments are presented in Figure 3 (data collected on both groups are included).

Alpha and beta angles of the UT on the closed eyelid were measured (Figure 1(b,c)) on 13 healthy volunteers (10 right eyes and three left eyes). Considering the workload in the eye clinic, we decided not to measure the alpha and beta angles of the UT on glaucoma patients. The results are presented in Table 3. The mean angle alpha in the case of the selected IOA segment simultaneously with EOA was 62.3° (SD = 4.8°). The mean angle alpha in the case of the identified edge of the ICA was 68.7° (SD = 21.0°); however, the difference was not statistically significant ($p = 0.30$). The mean angle beta in the case of the identified IOA segment simultaneously with EOA was 90.3° (SD = 4.3°); it was 99.4° (SD = 6.3°) for the identified ICA edge. The difference was statistically significant ($p = 0.0002$).

The relative UT positions on the closed eyelid in the case of the identified ICA edge and IOA segment selected simultaneously with the EOA were registered on 33 glaucomatous eyes and 33 healthy eyes. Using the average adult human orbit geometry, we estimated that the UT surface in all the cases of

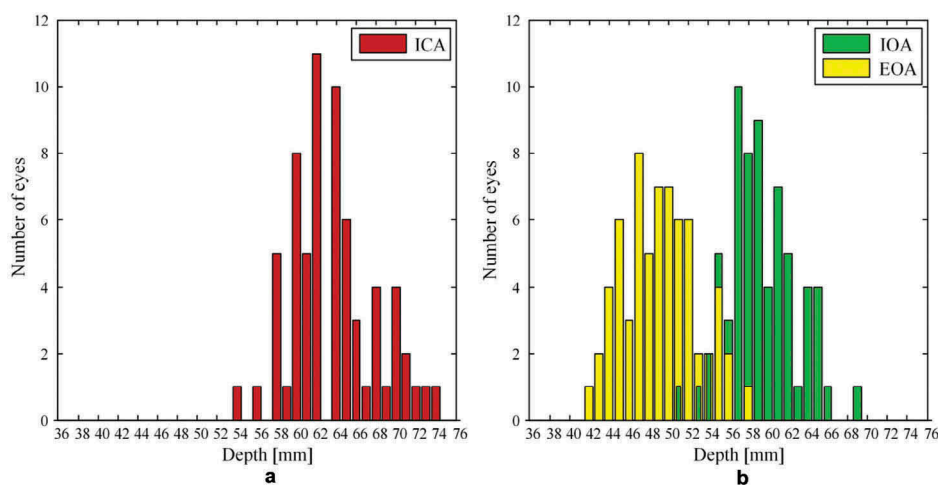


Figure 2. Distribution graphs of (a) identified depths of the internal carotid artery (ICA) edge (b) depths of the intracranial segment of the ophthalmic artery (IOA) selected simultaneously with the extracranial segment of the ophthalmic artery (EOA). Data collected on 25 high tension glaucoma patients (14 right eyes and 19 left eyes) and 23 healthy volunteers (20 right eyes and 13 left eyes) are included.

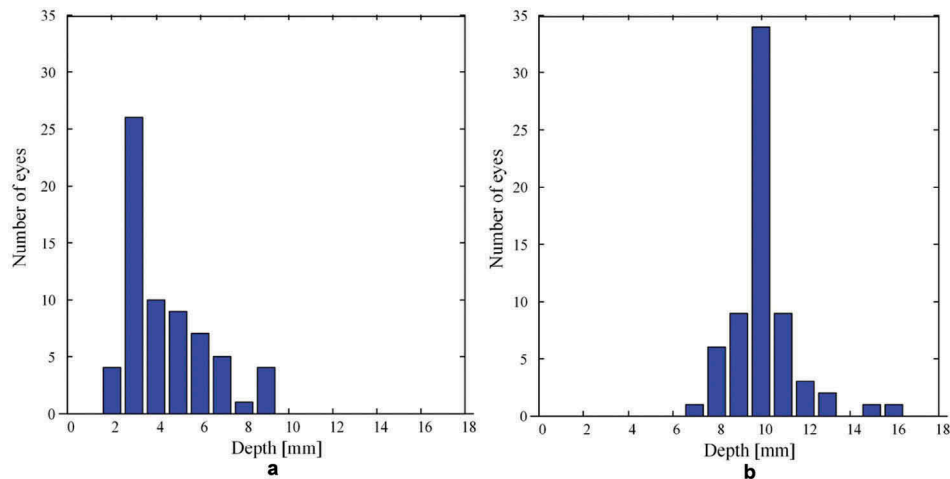


Figure 3. Distribution graphs of (a) distances between the identified edge of the internal carotid artery (ICA) and the selected depth of the intracranial segment of the ophthalmic artery (IOA) (ICA-IOA) (b) distances between the selected depth of the IOA and the extracranial segment of the ophthalmic artery (EOA) (IOA-EOA). Data collected on 25 high tension glaucoma patients (14 right eyes and 19 left eyes) and 23 healthy volunteers (20 right eyes and 13 left eyes) are included.

Table 3. Angles of the ultrasonic transducer on the closed eyelid in the case of the identified edge of the ICA and IOA segment selected simultaneously with the EOA in healthy volunteers.

No. of healthy volunteers	Eye	IOA and EOA		ICA edge	
		Alpha,°	Beta,°	Alpha,°	Beta,°
1	R	59.0	89.0	68.5	96.5
2	L	59.5	92.8	54.0	105.5
3	L	64.0	88.5	50.5	102.0
4	R	69.0	85.5	50.0	93.5
5	L	67.5	88.0	27.7	93.0
6	R	68.5	91.0	55.0	104.0
7	R	57.0	90.0	94.0	102.0
8	R	63.5	100	98.0	108.0
9	R	66.0	85.0	71.5	107.5
10	R	62.5	91.0	98.0	99.5
11	R	60.0	97.5	74.0	88.0
12	R	61.0	90.5	74.5	93.0
13	R	52.5	85.0	77.5	103.0
MEAN		62.3	90.3	68.7	99.4
SD		4.8	4.3	21.0	6.3

Data are presented for each healthy volunteer separately, including all 13 volunteers and 13 examined eyes. Means \pm SD are also presented. R indicates the right eye; L, left eye; ICA edge, identified depth of the internal carotid artery edge from the closed eyelid; IOA, selected depth of the intracranial segment of the ophthalmic artery from the closed eyelid; EOA, selected depth of extracranial segments of the ophthalmic artery from the closed eyelid; alpha, angle between the longitudinal axis of the ultrasonic transducer and the frontal axis of a human head; beta, angle between the longitudinal axis of the ultrasonic transducer and the vertical axis of a human head.

simultaneously selected IOA and EOA segments falls into a window of 26 mm in width and 20 mm in height (Figure 4(a)). The UT surface in all the cases of the identified ICA edge falls into a window of 28 mm in width and 22 mm in height (Figure 4(b)).

4. Discussion

The distances of the identified arteries are measured from the external surface of the closed eyelid via

established TCD measurement methodology in clinical practice. However, in some cases, e.g. high tension glaucoma, the internal structures of the eyeball can be deformed by high intraocular pressure. Thus, distances measured from the surface of the closed eyelid of the identified arteries might be different than in normal cases. Distances between the ICA edge and IOA segment as well as distances between IOA and EOA segments should be selected independently from the thickness of the closed eyelid and patient-specific anatomical features of an eyeball and orbit before non-invasive ICP measurement.

Here, a method to simultaneously locate intracranial and extracranial segments of the OA beginning with ICA edge location was tested prospectively. According to the proposed location method, the depth at which the OA branches from the ICA should be identified (ICA edge) in the first place. The edge of the ICA should be kept as a reference depth, and the intracranial segment of the OA should be selected 3–5 mm away from the identified ICA edge. The range of depth of the selected extracranial segment of the OA should be 8–12 mm away from the selected IOA depth.

In this prospective study, the edge of the ICA as well as the IOA and EOA segments were located using a multi-depth TCD device (Vittamed 205) dedicated to non-invasive ICP measurements. The probability of selecting an IOA segment at a distance not more than 5 mm from the identified ICA edge was 74% (49 cases from 66). Although the IOA segment was not always selected according to the proposed depth range (3–5 mm away from the identified ICA edge) for the non-invasive ICP measurement, the maximum selected distance was 9 mm, which fits the potential range of the IOA distance according to anatomical studies 0.5–9.5 mm [18,20–22]. The probability of selecting an EOA

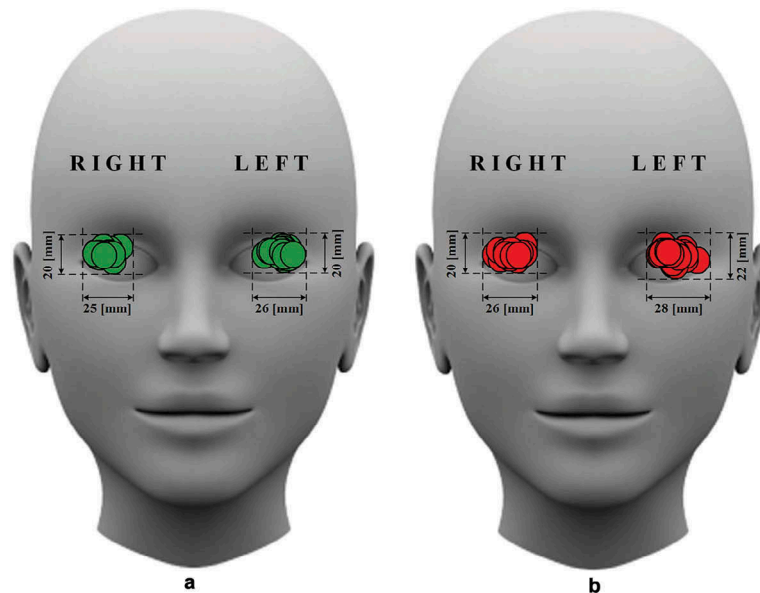


Figure 4. Relative positions of the ultrasonic transducer (UT) on the closed eyelid in the case of the located (a) intracranial segment of the ophthalmic artery simultaneously selected with the extracranial segment of the ophthalmic artery and (b) edge of the internal carotid artery. The width and height of the window within which the UT surface falls are indicated in millimetres.

segment according to the proposed depth range 8–12 mm from the selected IOA segment was 92% (61 cases from 66). However, the OA segment selected at a distance more than 12 mm from the selected IOA is in the range of the extracranial portion of the OA. This can be confirmed via the TCD spectral pattern. The reasons for selecting the IOA and EOA segments out of proposed distance range were that it was not possible to locate blood flow in such a distance range or the signal was too weak for the non-invasive ICP measurement.

Registered positions of the UT on the closed eyelid in the case of the identified ICA edge and IOA segment selected simultaneously with the EOA show that such positions are individual to each subject. This makes difficulties for the operator who manually locates OA segments for the non-invasive measurement of ICP.

However, the probability of finding the ICA edge and IOA simultaneously with the EOA for non-invasive ICP measurement is high by using the window of location areas defined in this study.

The results of this study reveal a statistically significant difference in the measured UT angles in the case of the identified ICA edge and IOA segment selected simultaneously with the EOA. We suggest that the operator who measures the ICP using this technique should expect to locate OA segments using different angles of UT compared with the case of the located ICA edge.

There are several limitations of our study. First, the investigation was conducted on only a limited number of adult subjects; therefore, the same ICA, IOA, and EOA segment location study might produce different results in children. Only Caucasian subjects were examined in both groups; therefore, we cannot assume that same results would be obtained in other races.

Additional medical imaging techniques such as magnetic resonance imaging (MRI) have not been used to support findings of multi-depth TCD. MRI can be used to identify abnormal anatomical structures around the ICA and OA, which can influence the accuracy of the location. Further studies that use MRI as an additional imaging technique are necessary to improve the accuracy and precision of identifying IOA and EOA segments.

This prospective study offers guidance for locating intracranial and extracranial segments of the ophthalmic artery to perform a reliable and non-invasive measurement of the intracranial pressure, which is important for the diagnosis and/or treatment of glaucoma.

5. Conclusions

We demonstrated that the location of the intracranial and extracranial segments of the ophthalmic artery can be achieved by identifying the edge of the internal carotid artery and by using that depth as a reference point for the reliable selection of IOA and EOA segments to non-invasively measure intracranial pressure absolute values.

Acknowledgments

The authors would like to express gratitude to the glaucoma patients and healthy volunteers who participated in this study. The authors would also like to express gratitude to Arminas Ragauskas who founded the non-invasive absolute ICP measurement method.

Disclosure statement

Mantas Deimantavicius, Evaldas Kalvaitis, Rolandas Zakelis and Laimonas Bartusis have received financial support from Vittamed UAB (Kaunas, Lithuania).

Funding

This work was supported by the European Social Fund [Grant number VP1-3.1-ŠMM-07-K-03-080].

ORCID

Yasin Hamarat  <http://orcid.org/0000-0002-1343-5068>

Laimonas Bartusis  <http://orcid.org/0000-0001-5835-5697>

References

- [1] Doherty CM, Forbes RB. Diagnostic lumbar puncture. *Ulster Med J.* 2014;83(2):93–102.
- [2] Bradley WG. Normal pressure hydrocephalus: new concepts on etiology and diagnosis. *AJNR Am J Neuroradiol.* 2000;21(9):1586–1590.
- [3] Akman-Demir G, Serdaroglu P, Taşci B. Clinical patterns of neurological involvement in Behçet's disease: evaluation of 200 patients. *Brain.* 1999;122(11):2171–2182.
- [4] Brain Trauma Foundation. Guidelines for the management of severe traumatic brain injury. *J Neurotrauma.* 2007;24(Suppl:1):1–106.
- [5] Andrews PJ, Citerio G, Longhi L, et al. NICEM consensus on neurological monitoring in acute neurological disease. *Intensive Care Med.* 2008;34(8):1362–1370.
- [6] Padayachy LC, Figaji AA, Bullock MR. Intracranial pressure monitoring for traumatic brain injury in the modern era. *Childs Nerv Syst.* 2010;26(4):441–452.
- [7] Berdahl JP, Fautsch MP, Stinnett SS, et al. Intracranial pressure in primary open angle glaucoma, normal tension glaucoma, and ocular hypertension: a case-control study. *Invest Ophthalmol Vis Sci.* 2008;49(12):5412–5418.
- [8] Berdahl JP, Allingham RR, Johnson DH. Cerebrospinal fluid pressure is decreased in primary open-angle glaucoma. *Ophthalmology.* 2008;115(5):763–768.
- [9] Siaudvytyte L, Januleviciene I, Ragauskas A, et al. The difference in translaminar pressure gradient and neuroretinal rim area in glaucoma and healthy subjects. *J Ophthalmol.* 2014 [cited 2017 Aug 21]; [5]. DOI:10.1155/2014/937360
- [10] Lin CM, Lin JW, Tsai JT, et al. Intracranial pressure fluctuation during hemodialysis in renal failure patients with intracranial hemorrhage. In: Chiu WT, Chiang YH, Kao MC, et al., editors. *Reconstructive neurosurgery.* Vienna: Springer Vienna; 2008. p. 141–144.
- [11] Ozturk T. Risks associated with laparoscopic surgery. In: Shamsa A, editor. *Advanced laparoscopy.* Rijeka: InTech; 2011. p. 1–26.
- [12] Aaslid R, Markwalder TM, Nornes H. Noninvasive transcranial Doppler ultrasound recording of flow velocity in basal cerebral arteries. *J Neurosurg.* 1982;57(6):769–774.
- [13] Naqvi J, Yap KH, Ahmad G, et al. Transcranial Doppler ultrasound: a review of the physical principles and major applications in critical care. *Int J Vasc Med.* 2013 [cited 2017 Aug 21]; [13]. DOI:10.1155/2013/629378
- [14] Cardim D, Robba C, Bohdanowicz M, et al. Non-invasive monitoring of intracranial pressure using transcranial Doppler ultrasonography: is it possible? *Neurocrit Care.* 2016;25(3):473–491.
- [15] Ragauskas A, Daubaris G, Dziugys A, et al. Innovative non-invasive method for absolute intracranial pressure measurement without calibration. *Acta Neurochir Suppl.* 2005;95:357–361.
- [16] Ragauskas A, Matijosaitis V, Zakelis R, et al. Clinical assessment of noninvasive intracranial pressure absolute value measurement method. *Neurology.* 2012;78(21):1684–1691.
- [17] Ragauskas A, Bartusis L, Piper I, et al. Improved diagnostic value of a TCD-based non-invasive ICP measurement method compared with the sonographic ONSD method for detecting elevated intracranial pressure. *Neurol Res.* 2014;36(7):607–614.
- [18] Michalinos A, Zogana S, Kotsiomititis E, et al. Anatomy of the ophthalmic artery: a review concerning its modern surgical and clinical applications. *Anat Res Int.* 2015 [cited 2017 Aug 21]; [8]. DOI:10.1155/2015/591961
- [19] Bathala L, Mehndiratta MM, Sharma VK. Transcranial doppler: technique and common findings (part 1). *Ann Indian Acad Neurol.* 2013;16(2):174–179.
- [20] Hayreh SS, Dass R. The ophthalmic artery: I. Origin and intra-cranial and intra-canalicular course. *Br J Ophthalmol.* 1962;46(2):65–98.
- [21] Jiménez-Castellanos J, Carmona A, Castellanos L, et al. Microsurgical anatomy of the human ophthalmic artery: a mesoscopic study of its origin, course and collateral branches. *Surg Radiol Anat.* 1995;17(2):139–143.
- [22] Erdogmus S, Govsa F. Anatomic features of the intracranial and intracanalicular portions of ophthalmic artery: for the surgical procedures. *Neurosurg Rev.* 2006;29(3):213–218.
- [23] Alexandrov AV, Sloan MA, Wong LK, et al. Practice standards for transcranial Doppler ultrasound: part I – test performance. *J Neuroimaging.* 2007;17(1):11–18.
- [24] Kassab MY, Majid A, Farooq MU, et al. Transcranial Doppler: an introduction for primary care physicians. *J Am Board Fam Med.* 2007;20(1):65–71.
- [25] Hu HH, Luo CL, Sheng WY, et al. Transorbital color Doppler flow imaging of the carotid siphon and major arteries at the base of the brain. *AJNR Am J Neuroradiol.* 1995;16(3):591–598.
- [26] René C. Update on orbital anatomy. *Eye.* 2006;20(10):1119–1129.
- [27] Dobrovat B, Popescu R, Nemtoi A, et al. Orbital trauma: from anatomy to imaging patterns – a pictorial review. *Rom Neurosurg.* 2011;18(4):525–532.